

Generating Likely Counterfactuals Using Sum-Product Networks

Jiří Němeček, Tomáš Pevný & Jakub Mareček

January 26, 2024

Abstract

Due to user demand and recent regulation (GDPR, AI Act), decisions made by AI systems need to be explained. These decisions are often explainable only *post hoc*, where counterfactual explanations are popular. The question of what constitutes the best counterfactual explanation must consider multiple aspects, where “distance from the sample” is the most common. We argue that this requirement frequently leads to explanations that are unlikely and, therefore, of limited value. Here, we present a system that provides high-likelihood explanations. We show that the search for the most likely explanations satisfying many common desiderata for counterfactual explanations can be modeled using mixed-integer optimization (MIO). In the process, we propose an MIO formulation of a Sum-Product Network (SPN) and use the SPN to estimate the likelihood of a counterfactual, which can be of independent interest. A numerical comparison against several methods for generating counterfactual explanations is provided.

1 Introduction

There is no doubt that the use of artificial intelligence (AI) is increasing. Consequently, a better understanding of the AI models deployed is needed, especially in high-risk scenarios [10]. Understanding AI models is usually seen through the lens of trustworthy and explainable AI (XAI), which is concerned with techniques that help people understand, manage, and improve trust in AI models [17, 6, 5]. Explanations also serve an important role in debugging models to ensure that they do not rely on spurious correlations and traces of processing correlated with labels, such as timestamps.

In a *post-hoc* explanation, a vendor of an AI system provides an individual user with a personalized explanation of an individual decision made by the AI system, improving the model’s trustworthiness [24, 27]. In this context, personalized explanations are often called local explanations because they explain the model’s decision locally, around a given sample, such as one person’s input. Local explanations thus provide information relevant to the user without revealing global information about the model, regardless of whether the model is interpretable *a priori*. Consider, for example, credit decision-making in financial services. The models utilized need to be interpretable *a priori*, cf. Equal Credit Opportunity Act in the US [11] and related regulation [12, 13].

in the European Union, but an individual who is denied credit may still be interested in a personalized, local explanation.

A well-known example of local explanations is the counterfactual explanation (CE). CE answers the question, “How should a sample be changed to obtain a different result?” [41]. In the example of credit decision-making, a denied client might ask what they should do to obtain the loan. The answer would take the form of a CE. For example, “Had your annual income been \$10,000 higher and had you spent \$1,000 less every month, your application would have been successful”. As illustrated, CE can be easily understood [7, 16]. However, their usefulness is influenced by many factors [16], including validity, similarity, sparsity, diversity, actionability, causality, and plausibility.

Here, we focus on the plausibility of counterfactual explanations. In the example above, reducing spending might mean leaving an area with a high cost of living. This might be difficult to combine with finding a better-paying job to increase the annual income, making the whole counterfactual implausible. Instead, moving to the capital may make it possible to double the annual income while increasing the monthly expenses somewhat. Despite the larger distance from the decision boundary, this latter CE may be more plausible. More broadly, the question of plausibility is interesting because it does not have a clear definition. Guidotti’s definition is CE not being an outlier, and he measures it as mean distance to data [16]. A common approach to the plausibility of CE uses (Conditional) Variational Auto Encoders [22, 35, 16] in likelihood estimation. However, variational auto-encoders provide only a lower bound on likelihood and are intractable models of probability distributions [22, 26], which means that one cannot efficiently compute the exact likelihood or marginalize variables with polynomial-time complexity with respect to the size of the encoder [8]. Therefore, we ask how best to consider tractable probabilistic models in this context.

Our Contribution We propose a method for Likely Counterfactual Explanations (LiCE) using Sum-Product Networks (SPN) [37] to estimate the likelihood of a counterfactual, and thus plausibility, while satisfying most other common desiderata modeled within mixed-integer optimization (MIO). This combines the traditions of tractable probabilistic models with MIO.

MIO has been used to search for CEs before the term CE was first used [9]. MIO has favorable properties of being model-agnostic, at least as long as the model can be formulated in MIO, and satisfying validity by design. Russell [39] considered generating multiple explanations using a custom MIO solver. One can also implement various constraints [e.g. 28]. At the same time, this improves upon the early uses of tractable probabilistic models in CE generation, such as [1], which estimate a Gaussian Mixture Model and which we refer to as PlaCE (Plausible CEs), where PlaCE is limited in its inability to handle categorical features. This limitation of PlaCE is inherent in its Gaussian Mixture Model design.

The advantage can be illustrated with a simple example on the so-called Adult data set [3], which is certainly not representative of datasets utilized in real-world credit decision-making but remains an easy-to-understand proxy for credit decision-making, which has been utilized by much of the previous research on CEs. See Figure 1 for a

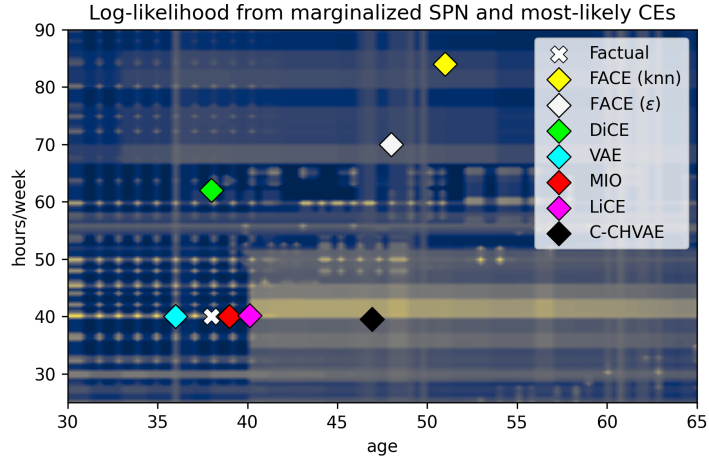


Figure 1: The heatmap shows the marginalized likelihood distribution of the Adult dataset into a 2-dimensional space of hours/week and age features. The factual (white cross) and CEs are projected to the two dimensions. The factual is classified as having a low income. Most CE methods choose distant points with poor likelihood. The proposed method (LiCE) strikes a balance between likelihood and proximity. For methods capable of outputting multiple CEs (DiCE, VAE, MIO, LiCE), we show the most likely out of 10, based on the SPN.

plot where CEs produced by a number of methods considering diversity or plausibility of CE are compared against the factual (white cross) in the plane, where the horizontal axis represents the age (which seems hard to decrease) and where the vertical axis is the number of hours worked per week. The heatmap corresponds to the likelihood of the CE, evaluated using an SPN trained on the randomly sampled training set (80% of the dataset). Notice that the higher likelihood of integral values of change in the age is an artifact of the training data allowing only for integral values of the age. For example, FACE [38] suggests doubling the number of hours worked per week. The most plausible explanation produced by DiCE [32] suggests increasing the number of hours worked per week by 22. C-CHVAE [35] suggests waiting for eight years, while VAE unhelpfully suggests applying two years ago. In contrast, LiCE works with the constraint on the age being a non-decreasing quantity and finds a CE comprising waiting for two years.

In particular, we present:

- Sum-Product Network as a measure of plausibility of CE, with a MIO formulation.
- LiCE method for the generation of CE. A MIO model that can be constrained by or optimized with respect to the most common desiderata regarding CE generation, including plausibility.
- A numerical comparison of several CE techniques that optimize plausibility.

Notation used Throughout the paper, we consider a classification problem where the dataset \mathcal{D} is a set of 2-tuples $(\mathbf{x}, y) \in \mathcal{D}$. Each input vector $\mathbf{x} \in \mathcal{X} \subseteq \mathbb{R}^P$ consists of P features and is taken from the input space \mathcal{X} that can be smaller than P -dimensional real space (e.g., can contain categorical values). x_j is the value of the j th feature of the sample \mathbf{x} . We have C classes and describe the set of classes $[C] = \{1, \dots, C\}$. $y \in [C]$ is the true class of the sample \mathbf{x} . Finally, we have a classifier $h(\mathbf{x}) = \hat{y} \in [C]$ that predicts the class \hat{y} for the sample \mathbf{x} . Our goal is to find a set of M counterfactuals $\mathcal{C}_{\mathbf{x}} = \{\mathbf{x}'_{(1)}, \dots, \mathbf{x}'_{(M)}\}$ for a given \mathbf{x} . Note that the bold \mathbf{x}' means that the subscripts refer to indices of counterfactual instances within $\mathcal{C}_{\mathbf{x}}$ rather than a feature index. Further details about the notation are in Appendix A.

2 Related Work

There is a plethora of work on the search for CEs, as recently surveyed [16, 6, 5, e.g.]. See [24, cf. Table 1] for a one-page overview. In our overview, we will focus on methods that support both categorical and continuous-valued features, with objectives related to the plausibility, actionability, or likelihood of the CE and methods utilizing MIO.

Historically, a number of terms have been used for related approaches. Focusing on approaches that use MIO, pioneering work [9] considered classifiers based on additive tree models and extracted an optimal plan to change a given input to a desired class at a minimum cost, calling the problem “optimal action extraction” (OAE). In parallel, similar approaches have been developed under the banner of “actionable recourse” [40] or “algorithmic recourse” [24, 25]. Developing upon this, [25] distinguish between contrasting explanations and consequential explanations, where actions are modeled explicitly in a causal model. We will use the term counterfactual explanations, popularized by [41, e.g.].

2.1 Counterfactuals

We define a counterfactual explanation in accordance with previous works as $\mathbf{x}' \in \mathcal{X}$ such that $h(\mathbf{x}) \neq h(\mathbf{x}')$ and the distance between \mathbf{x}' and \mathbf{x} is in some sense minimal [16, 41]. We refer to \mathbf{x} as factual and \mathbf{x}' as a counterfactual. As mentioned before, there are many desiderata regarding the properties of CEs. Following [16], the common desiderata include:

- *Validity.* \mathbf{x}' should be classified differently than \mathbf{x}
- *Similarity.* \mathbf{x}' should be similar (close) to \mathbf{x}
- *Sparsity.* \mathbf{x}' should minimize the number of changed features compared to \mathbf{x} , i.e., minimize $\|\mathbf{x}' - \mathbf{x}\|_0$
- *Diversity.* Each $\mathbf{x}'_{(m)} \in \mathcal{C}_{\mathbf{x}}$ should be as different as possible from any other CE in the set, ideally by proposing changes in different features. For example,

one CE recommends increasing the income; another one should recommend decreasing the loan amount instead. An important example of a CF library aiming for diversity is DiCE [32].

- *Discriminative power.* In simple terms, \mathbf{x}' should make it clear to humans why the change causes a change in classification. We disregard discriminative power in our proposed method because it depends more on the decision boundary of the model rather than the counterfactual measure. Our method can produce counterfactuals on the decision boundary, suggestive of the neighborhood of a factual. It can also produce more likely counterfactuals farther away from the boundary, based on the parameters.
- *Actionability.* A counterfactual should change only features that can be influenced in reality. It should also change them correctly, such as only increasing the age.
- *Causality.* Given that we know some causal relationships between the features, the generated CEs should follow them. For example, if \mathbf{x}' contains a decrease in the total loan amount, the number of payments or their amount should also decrease.
- *Plausibility.* While computing the probability of a CE in a given probabilistic model may be NP-Hard, we would like to produce high-probability CEs that would not be outliers in the dataset \mathcal{D} [16, 45]. Therefore, we estimate the likelihood of \mathbf{x}' , for instance using autoencoders [35, 28, e.g.] or by Gaussian Mixture Models [1] or by probabilistic circuits such e.g., Sum-Product Networks (SPNs) in this paper, and promote CEs with the highest estimated likelihood.

2.2 Mixed-Integer Optimiation

Mixed-integer optimization (MIO, [43]) is a powerful framework for modeling and solving optimization problems, where some decision variables take values from a discrete set while others are continuously valued. Non-trivially, the problem is in NP [33] and is NP-Hard, in general. There has been fascinating progress in the field in the past half-century [4]. State-of-the-art solvers based on the branch-and-bound-and-cut approach can often find global, certified optima for instances with millions of binary variables within hours, while there are pathological instances on under a thousand variables whose global optima are still unknown. Naturally, MIO is widely used in areas of machine learning, where both discrete and continuous decision variables need to be optimized over jointly [20, e.g.].

In counterfactual reasoning, where we often need to consider both categorial and continuous-valued features, MIO has been used since the early days [9, 40, 39, 23, 34, 30, 21]. A crucial advance has been Russell’s mixed polytope formulation [39], which neatly combines categorical and continuous values. A feature j takes a continuous value from the $[L_j, U_j]$ range or one of K_j distinct categorical values. This is useful for modeling data with missing features, especially when there is a description of why the value is missing [39]. To model the mixed polytope [39] of a counterfactual for the

feature j , we create a one-hot encoding for K_j discrete values into binary variables $d_{j,k}$ and a continuous variable c_j with a binary indicator variable d_j^{cont} equal to 1 when the feature takes a continuous value. In summary:

$$\sum_{k=1}^{K_j} d_{j,k} + d_j^{\text{cont}} = 1 \quad (1)$$

$$c_j = F_j d_j^{\text{cont}} - l_j + u_j \quad (2)$$

$$0 \leq l_j \leq (F_j - L_j) d_j^{\text{cont}} \quad (3)$$

$$0 \leq u_j \leq (U_j - F_j) d_j^{\text{cont}} \quad (4)$$

$$d_j^{\text{cont}}, d_{j,k} \in \{0, 1\} \quad \forall k \in [K_j], \quad (5)$$

where F_j is either the original value x_j or the median value if the factual x_j has a categorical value instead. The computation of counterfactual c_j in (2) uses two non-negative variables, l_j and u_j , representing the decrease and increase in the continuous value, respectively. This construction facilitates the computation of the absolute difference from the factual. Since we minimize their (weighted) sum, at least one of them will always equal 0. [39]

2.3 Sum-Product Networks

Probabilistic circuits (PCs) [8] are tractable probabilistic models (or rather, computational graphs) that support exact probabilistic inference and marginalization in linear time of their representation size. Probabilistic circuits are defined by a tuple $(\mathcal{G}, \psi, \theta)$, where $\mathcal{G} = (\mathcal{V}, \mathcal{E})$ is a Directed Acyclic Graph (DAG) defining the computation model, a scope-function $\psi : \mathcal{V} \rightarrow 2^{[P]}$ defines a subset of features over which the node defines its distribution, and a set of parameters θ . To simplify the notation, we define a function $\text{pred}(n)$, giving a set of children (predecessors) of a computation node n .

An important subclass of PCs are Sum-Product Networks (SPNs), which restrict PCs such that the inner (non-leaf) nodes can be only sums and products. We denote the set of sum nodes \mathcal{V}^Σ and product nodes \mathcal{V}^Π .

Leaf node $n^\text{L} \in \mathcal{V}^\text{L} = \{n \mid \text{pred}(n) = \emptyset\}$ within SPNs takes a value O_{n^L} from a (tractable) distribution over its scope $\psi(n^\text{L})$ parametrized by θ_{n^L} .

Sum node $n^\Sigma \in \mathcal{V}^\Sigma$ has its value defined as

$$O_{n^\Sigma}(\mathbf{x}) = \sum_{a \in \text{pred}(n^\Sigma)} w_{a,n^\Sigma} \cdot O_a(\mathbf{x}),$$

where weights $w_{a,n^\Sigma} \geq 0$ and $\sum_{a \in \text{pred}(n^\Sigma)} w_{a,n^\Sigma} = 1$. The value of a sum node is thus a mixture of distributions defined by its children. The scope of each sum node must satisfy completeness (smoothness), i.e., it must hold that $\psi(a_1) = \psi(a_2) \forall a_1, a_2 \in \text{pred}(n^\Sigma)$.

Product node $n^\Pi \in \mathcal{V}^\Pi$ performs a product of probability distributions defined by its children, i.e., $O_{n^\Pi}(\mathbf{x}) = \prod_{a \in \text{pred}(n^\Pi)} O_a(x_{\psi(a)})$. The scope of product nodes must satisfy decomposability, meaning that the scopes of its children are disjoint,

i.e., $\bigcap_{a \in \text{pred}(n^\Pi)} \psi(a) = \emptyset$, but complete

$$\psi(n^\Pi) = \bigcup_{a \in \text{pred}(n^\Pi)} \psi(a).$$

The root node n^{root} (a node without parents) has the scope-function over all features, i.e., $\psi(n^{\text{root}}) = [P]$.

There are a variety of methods for training SPN [44], out of which we use a variant of LearnSPN [14] with k-means clustering, as implemented in the SPFlow library [31].

3 Our Method

We now present our model for Likely Counterfactual Explanations (LiCE). Combining the strictness and global properties of MIO with the likelihood modeling capabilities of SPNs, we create a model capable of satisfying most of the common desiderata for CEs. We assume that all continuous values are normalized to the range $[0, 1]$.

3.1 MIO formulations

Input encoding To encode the input vector, we extend the mixed polytope formulation [39], as explained in Eqs. 1–5 on page 6. The mixed polytope encoding works for purely continuous values by setting $K_j = 0$. For purely categorical features, the original implementation contained an issue. The first categorical value (represented by zero) was mapped to the continuous variable. This seems to have worked fine for the logarithmic regression [39], but it failed on non-monotone neural networks leading to non-binary outputs. This was corrected by replacing the continuous variable c_j with another binary decision variable, making it a standard one-hot encoding. For a more in-depth explanation of the mixed polytope, we refer to the paper introducing the method [39]. As an input to the neural network, we concatenate all variables c_j and $d_{j,k}$ (but not d_j^{cont}) into a single vector. With some abuse of the notation, we denote this vector \mathbf{x}' . We further use \mathcal{X} for the space of encoded inputs and P for the number of encoded variables, when there is no risk of confusion.

Model encoding To encode the classification model, we use the Gurobi Machine Learning library [2024]. It enables simple encoding of various machine-learning models, including neural networks and gradient-boosted trees. In our experiments, we used a simple neural network with ReLU activations. Linear combinations in layers are modeled directly, while ReLUs are modeled using general max constraints, which are mixed-integer representable using linear and SOS1 constraints [18]. We now show that we can model various desiderata as constraints in the MIO formulation. Given that they are constraints, we are certain that each generated counterfactual satisfies them.

Validity Let $h^{\text{raw}} : \mathcal{X} \rightarrow \mathcal{Z}$ be the neural network model $h(\cdot)$ without activation at the output layer. $h^{\text{raw}}(\mathbf{x}')$ is the output we obtain from the model implementation.

Assuming we have a binary classification task ($C = 2$), a neural network typically has a single output neuron ($\mathcal{Z} = \mathbb{R}$). A sample \mathbf{x} is classified based on whether the raw output is above or below 0, i.e., $h(\mathbf{x}) = \mathbb{1}\{h^{\text{raw}}(\mathbf{x}) \geq 0\}$. Therefore, we can model the decision by selecting a multiplication with the desired sign $\sigma \in \{-1, 1\}$

$$\sigma h^{\text{raw}}(\mathbf{x}') \geq \tau, \quad (6)$$

where $\tau \geq 0$ is a margin that can be set to ensure a higher certainty of the decision, improving the reliability and robustness of the CE.

For $C > 2$ classes, the raw output has C dimensions ($\mathcal{Z} = \mathbb{R}^C$), and the classifier assigns the class equal to the index of the highest value, i.e., $h(\mathbf{x}) = \arg \max_{k \in [C]} h^{\text{raw}}(\mathbf{x})_k$. Let \hat{y}' be the desired counterfactual class. The validity constraint is then

$$h^{\text{raw}}(\mathbf{x}')_{\hat{y}'} - h^{\text{raw}}(\mathbf{x}')_k \geq \tau \quad \forall k \in [C] \setminus \{\hat{y}'\}. \quad (7)$$

Note that we can also implement a version where we do not know the counterfactual class \hat{y}' in advance by the following

$$\begin{aligned} g_k = 1 &\implies h^{\text{raw}}(\mathbf{x}')_k - h^{\text{raw}}(\mathbf{x}')_{\hat{y}} \geq \tau \quad \forall k \in [C] \setminus \{\hat{y}\} \\ g_k = 0 &\implies h^{\text{raw}}(\mathbf{x}')_k - h^{\text{raw}}(\mathbf{x}')_{\hat{y}} \leq \tau \quad \forall k \in [C] \setminus \{\hat{y}\} \\ &\sum_{k \in [C] \setminus \{\hat{y}\}} g_k \geq 1, \end{aligned} \quad (8)$$

where \implies can be seen either as an indicator constraint or as an implication [42], g_k is equal to 1 if and only if class k has a higher value than the factual class \hat{y} in the raw output. The sum then ensures that at least one other class has a higher value.

A wide variety of constraints ensuring validity are possible. For example, we can ensure that the factual class has the lowest score by setting $\sum_{k \in [C] \setminus \{\hat{y}\}} g_k \geq C - 1$, or we could enforce a custom order of classes.

Similarity and Sparsity To ensure similarity of the counterfactual, we follow [41, 39] and use the somewhat non-standard $\|\cdot\|_{1,\text{MAD}}$ norm, weighed by inverse Median Absolute Deviation (MAD):

$$\begin{aligned} \|\mathbf{x}\|_{1,\text{MAD}} &= \sum_{j=1}^P \left| \frac{x_j}{\text{MAD}_j} \right| \\ \text{MAD}_j &= \text{median}_{(\mathbf{x}, \cdot) \in \mathcal{D}} (|x_j - \text{median}_{(\mathbf{x}, \cdot) \in \mathcal{D}} (x_j)|). \end{aligned} \quad (9)$$

This metric also improves sparsity and adds scale invariance that is robust to outliers [39].

To constrain sparsity further, we can set an upper bound S on the number of features

changed

$$\begin{aligned}
\sum_j s_j &\leq S \\
s_j &\geq 1 - d_{j,f_j} & \forall j \in [P] \\
s_j &\geq d_{j,k} & \forall j \in [P], \forall k \in [K_j] \setminus \{f_j\} \\
s_j &\geq l_j + u_j & \forall j \in [P] \\
s_j &\in \{0, 1\} & \forall j \in [P],
\end{aligned} \tag{10}$$

where we use the binary value s_j that equals 1 if the j -th feature changed, the f_j is the categorical value of attribute j of the factual (if applicable).

Actionability and Causality Both actionability and causality depend on prior knowledge of the data, and can be phrased as logical constraints. In the case of actionability, the constraint is simply $x_j = x'_j$ for all non-actionable features j . However, we do not need to introduce additional constraints to the model. Rather, we set the input value as a parameter, omitting the mixed polytope encoding altogether.

In causality, the constraints are in the form of implications [28]. Consider the following example of a causal relation R . If feature j increases its value, another feature e must decrease. For continuous ranges, this is formulated as

$$\begin{aligned}
r &\geq u_j - l_j \\
l_e &\geq r\epsilon_e \\
u_e &\leq 1 - r \\
r &\in \{0, 1\},
\end{aligned} \tag{11}$$

where ϵ_e is a minimal change in the value of feature e and r equals 1 if the relation R is active. In the case when the features are categorical, we can assume that their values are ordered by indices and use:

$$\begin{aligned}
r &\geq \sum_{k=f_j+1}^{K_j} d_{j,k} \\
r &\leq \sum_{k=1}^{f_e} d_{e,k} \\
r &\in \{0, 1\},
\end{aligned} \tag{12}$$

where f_j is the categorical value of the factual in feature j . Naturally, one can see that we can use any combination of increasing/decreasing values in continuous and categorical feature spaces. We can also use similar constraints to model inherently increasing values, such as age. We simply replace the variable r by 1.

Diversity and Robustness The diversity of CEs generated by MIO is discussed in depth by [39]. While his approach can be applied to our model too, here we generate a set of top- M counterfactuals closest to the global optimum. Instead of a single

counterfactual, the solver thus returns (up to) M counterfactuals closest to the global optimum within some distance range. This distance is defined in terms of the objective function, which is weighed distance in our case. In other words, we search for a set $\mathcal{C}_x = \{x'_{(1)}, \dots, x'_{(M)}\}$ counterfactuals that have a distance similar to the factual.

Let x'^* be the closest CE satisfying all other constraints; we set a parameter ρ that represents the relative distance of all CEs to the x'^* leading to the generation of set

$$\mathcal{C}_x = \{x' \mid \|x - x'\|_{1,\text{MAD}} \leq (1 + \rho) \cdot \|x - x'^*\|_{1,\text{MAD}}\}.$$

Optionally, we may disregard the relative distance, and parameterize the search only with M instead, where M is the number of closest CEs we want. Later, we can sift through the set \mathcal{C} , looking for a diverse subset or a subset of the most likely CEs, which is one of the methods we examine (called MIO in Section 4).

Regarding the robustness of the counterfactuals, Artelt *et al.* show that finding plausible CEs indirectly improves the robustness [2]. Thus, we do not add any further constraints to the model, despite this being a viable option [29, e.g.].

Plausibility Finally, we address plausibility. Artelt and Hammer are the first to use a tractable model to approximate the likelihood of a counterfactual [1]. Their formulation approximates a GMM with a quadratic term and uses a general convex optimization solver. Instead, we propose to use a trained SPN (see below) to estimate the likelihood of a counterfactual. In experiments, we use it to select the most likely of counterfactuals, generated using various methods. Furthermore, we propose a MIO formulation for estimates bounding the SPN likelihood from above and from below.

Sum-Product Network Since the multiplication of variables in the product nodes is not desirable for linear formulations and numerical stability is an issue for MIO solvers, we perform all computations in the log space. Also note that for the SPN computation, we add the counterfactual class \hat{y}' as an additional input feature $x'_{P+1} = \hat{y}'$.

We consider the probability distributions of any leaf $n \in \mathcal{V}^L$ to be a histogram on a single feature j , i.e., $\psi(n) = \{j\}$. The interval of possible values of x'_j is split into B_n bins, delimited by $B_n + 1$ breakpoints denoted $t_{n,i}$, $i \in [B_n + 1]$. Because modeling that a variable belongs to a union of intervals is simpler than an intersection, we consider variables $\bar{b}_{n,i}$ that equal 1 if and only if the value x'_j does *not* belong to the interval $[t_{n,i}, t_{n,i+1})$. This leads to a set of constraints

$$\bar{b}_{n,i} \geq t_{n,i} - x'_j \quad \forall n \in \mathcal{V}^L, \forall i \in [B_n] \quad (13)$$

$$\bar{b}_{n,i} \geq x'_j + \epsilon_j - t_{n,i+1} \quad \forall n \in \mathcal{V}^L, \forall i \in [B_n] \quad (14)$$

$$\sum_{i=1}^{B_n} \bar{b}_{n,i} = B_n - 1 \quad \forall n \in \mathcal{V}^L \quad (15)$$

$$o_n = \sum_{i=1}^{B_n} (1 - \bar{b}_{n,i}) \ln q_{n,i} \quad \forall n \in \mathcal{V}^L \quad (16)$$

$$\bar{b}_{n,i} \in \{0, 1\} \quad \forall n \in \mathcal{V}^L, \forall i \in [B_n], \quad (17)$$

where $q_{n,i}$ is the likelihood value in a bin i and o_n is the output value of the leaf node n and takes negative values. ϵ_j is again the minimal change in the feature j and ensures that we consider an open interval on one side. We use the fact that all values x_j (thus also $t_{n,i}$) are in the interval $[0, 1]$. Eq. 13 sets $\bar{b}_{n,i} = 1$ if $x'_j < t_{n,i}$ and Eq. 14 sets $\bar{b}_{n,i} = 1$ for values on the other side of the bin $x'_j \geq t_{n,i+1}$. Eq. 15 ensures that a single bin is chosen and Eq. 16 sets the output value to the log value of the bin that \mathbf{x}' belongs to. This implementation of bin splitting is inspired by the formulation of interval splitting in piecewise function fitting [15].

We assume that the bins cover the entire space, which we can ensure by adding at most 2 bins on both sides of the interval. The formulation is valid also for categorical features, by mapping them back to their numerical representations. However, we can also use the $d_{j,k}$ variables directly by setting $\bar{b}_{n,i} \leq 1 - d_{j,k}$, $\psi(n) = \{j\}$ when k represents a categorical value belonging to bin i .

Having obtained the output of the leaf nodes, we move to inner nodes. Each node n produces an output o_n combining the outputs o_a , $a \in \mathcal{A}_n = \text{pred}(n)$ of its predecessors. Consider now a product node $n \in \mathcal{V}^\Pi$, with output defined as a product of predecessor outputs. Since we consider all computations in log space, this translates to

$$o_n = \sum_{a \in \mathcal{A}_n} o_a \quad \forall n \in \mathcal{V}^\Pi. \quad (18)$$

So far, we have produced the exact output values. For sum nodes, however, this is no longer possible. Sum node $n \in \mathcal{V}^\Sigma$ is defined as a sum of predecessor a outputs, each weighted by $w_{a,n}$. In log space, the weighted sum would translate to $o_n^* = \log \sum_{a \in \mathcal{A}_n} w_{a,n} \exp(o_a)$, which we cannot model easily. To approximate this expression, we notice that $w_{a,n} \exp(o_a) = \exp(o_a + \log w_{a,n})$, and that we can approximate $\log \sum \exp(z)$ by $\max z$. Specifically, let $z_a = o_a + \log w_{a,n}$ and we bound

$$\begin{aligned} \max_{a \in \mathcal{A}_n} z_a &= \log \exp(\max_{a \in \mathcal{A}_n} z_a) \leq \log \sum_{a \in \mathcal{A}_n} \exp(z_a) = o_n^* \\ &\leq \log(|\mathcal{A}_n| \exp(\max_{a \in \mathcal{A}_n} z_a)) \\ &= \log(|\mathcal{A}_n|) + \max_{a \in \mathcal{A}_n} z_a. \end{aligned}$$

That is: we can bound the true o_n^* from below, and the error in the estimate will be at most logarithm of the number of predecessors. Putting this into our formulation, we once again utilize the general max constraint, linearized by the solver

$$o_n = \max_{a \in \mathcal{A}_n} (o_a + \log w_{a,n}) \quad \forall n \in \mathcal{V}^\Sigma, \quad (19)$$

where o_n is in a conservative estimate of the true o_n^* as explained above. If we wanted to use the overestimation variant, we could easily add $\log |\mathcal{A}_n|$ to the estimate o_n .

Obtaining the SPN result means taking the o_{root} value of the root. We can plug this directly into the formulation. It could be added to the objective function with a multiplicative coefficient, but we opt for a fixed threshold, similarly to [1]. Let n^{root} be the root node, we add the constraint

$$o_{n^{\text{root}}} \geq \delta^{\text{SPN}}, \quad (20)$$

Method	Log-density on common factuals		Log-density on all factuals		% of CEs		Time
	Valid (17%)	Actionable (7%)	Valid	Actionable	Valid	Actionable	
DiCE	-25.27 ± 15.42	-23.81 ± 14.72	-31.58 ± 46.97	-31.65 ± 47.10	99.8%	99.2%	18.32s
VAE	-12.47 ± 1.08	-12.53 ± 0.98	-12.87 ± 2.36	-12.91 ± 2.57	77.8%	37.0%	0.04s
FACE (e)	-13.52 ± 4.42	-12.42 ± 1.77	-14.30 ± 5.78	-14.42 ± 6.16	48.8%	37.6%	8.25s
FACE (knn)	-13.31 ± 3.74	-12.85 ± 2.00	-13.82 ± 4.83	-14.01 ± 5.38	58.6%	43.0%	8.21s
C-CHVAE	-14.98 ± 2.07	-14.92 ± 2.34	-15.88 ± 2.54	-16.00 ± 2.72	60.2%	39.8%	0.79s
MIO	-12.95 ± 4.20	-11.82 ± 1.25	-15.93 ± 10.15	-15.93 ± 10.17	85.8%	85.4%	0.43s
LiCE	-12.09 ± 1.59	-11.72 ± 1.16	-12.52 ± 1.83	-12.52 ± 1.83	51.6%	51.6%	64.36s

Table 1: Mean log-density of counterfactual explanation based on an optimized KDE over a 5-fold cross-validation. Because each method sometimes fails, first two columns compare the methods on factuals for which *all* CE methods returned a (valid/actionable) counterfactual. As actionable CEs are considered only *valid* counterfactuals that also satisfy *actionability*. Because of a relatively low amount of common factuals (85 for valid and 36 for actionable out of 500), we presume them to be non-representative instances and show also the density for each method on all generated CEs. These are means over a varying number of factuals, shown in the next two columns. For comparison, median log-density of testing data was -12.64 . Time column shows mean computation time computed over all valid CEs of the respective method.

where δ^{SPN} is a hyperparameter of our method. Similarly to [1], we choose δ^{SPN} as the median log-likelihood of the training data, estimated by our SPN.

Full LiCE model In summary, our method uses:

$$\begin{aligned} \arg \min_{\mathbf{l}, \mathbf{u}, \mathbf{d}} & (\mathbf{l} + \mathbf{u})^\top \mathbf{v}^{\text{cont}} + (\mathbf{d} - \mathbf{d}^{\text{fact}})^\top \mathbf{v}^{\text{bin}} & (21) \\ \text{s.t.} & \text{ mixed-polytope conditions (1–5) hold} \\ & \text{validity constraint (one of (6–8)) holds} \\ & \text{SPN constraints (13–19) hold} \\ & \text{plausibility constraint (20) holds} \\ & \text{optionally other desiderata constr. (10–12) hold,} \end{aligned}$$

where \mathbf{l} , \mathbf{u} and \mathbf{d} represent the vectors obtained by concatenation of the parameters in Eqs. 1–5. The vector \mathbf{d}^{fact} is the vector of binary variables of the encoded factual \mathbf{x} . \mathbf{v}^{cont} and \mathbf{v}^{bin} represent weights for continuous and binary variables, respectively. In our case, the weights for feature j are $1/\text{MAD}_j$ and Eq. 21 corresponds Eq. 9.

4 Experiments

We aim to compare the plausibility of counterfactuals generated by a number of methods. For that purpose, we compare the density estimate using a Kernel Density Estimator (KDE) as performed by [1]. Similarly to them, KDE is trained on the same training data as all other models and has hyperparameters optimized using grid search.

From the test set, we sample 100 samples and find CEs. For methods that can output more samples (MIO, LiCE, DiCE, VAE), we find (at most) 10 CEs, test for validity and actionability, measure their quality using an SPN (we use the SPFlow library [31])

trained on the same training set, and select one with the highest estimated likelihood that is valid and actionable, or at least valid. If a method requires any prior training, we use the default hyperparameters and train it on the same training set. If a given method can take into account actionability and causality conditions, we enforce, for the sake of an example, non-actionability of changes of race and gender attributes, as well as all causal conditions as presented in [28].

We performed tests on a variant of the Adult data set [3]. We performed all experiments in a 5-fold cross-validation setting. Thus, we trained 5 variants of each model (except for KDE, where we trained one for each class, 10 in total).

Methods We compare the following CE methods:

- **MIO** represents our method without the SPN model directly formulated. We use all constraints described in Section 3, except for the hard constraint for sparsity in Eq. 10.
- **LiCE** is our proposed model. It is similar to MIP, with the additional plausibility constraint (Eq. 20) using the SPN.
- **DiCE** is a well-known method focusing on generating a diverse set of counterfactuals [32].
- **VAE** is a method using VAE. We use the implementation available in version 0.4 of the DiCE library, based on [28].
- **FACE** focuses on selecting a CE from the training set \mathcal{D} , rather than generating it from \mathcal{X} . It works by navigating a graph of the samples \mathbf{x} , where an edge exists between 2 samples if they are close (ϵ variant) or by connecting k nearest neighbours (knn variant) [38].
- **C-CHVAE** uses a Conditional VAE to search for plausible (they use the term *faithful*) CEs without the need for a metric in the original space [35].

PlaCE [1] does not have an implementation for Neural Networks, so we did not compare with it. We use the implementations of FACE and C-CHVAE provided in the CARLA library [36]. As a solver for MIO and LiCE, we use the Gurobi optimizer [2023]. The entire implementation, together with data, will be made open source. All experiments were run on a personal laptop.

Results The proposed LiCE method performs best with respect to the plausibility of CEs when measured by a Kernel Density Estimator (see all log-density values in the last row of Table 1). The method assessment holds even compared to the median log-density of -12.64 computed on the out-of-sample data. However, the plausibility constraint in LiCE means that around half of the factuals do not receive a valid counterfactual. That might be partly caused by other factors since MIO also does not generate all 100% of valid CEs. It could also be caused by numerical instabilities or infeasibility of the formulation because of, e.g., causality constraints.

Although DiCE is able to generate a valid and actionable counterfactual for almost all tested factuals, the counterfactuals generated are mostly poor in terms of plausibility, despite selecting the most likely out of 10.

Even though VAE also generates 10 CEs, it is the fastest method by an order of magnitude. In addition, VAE achieves plausibility comparable to LiCE. This effectiveness is contrasted with the method having the worst retrieval rate of actionable CEs of all methods.

The FACE method has a quite poor retrieval rate of actionable CEs as well. This might be caused by a combination of selecting samples that are then misclassified by the model and not finding a CE on the graph. Despite the use of samples from the data as CEs, the density is not as high as in the case of LiCE and VAE, which is likely due to outlier samples used as CEs.

Despite its use of Conditional VAE, C-CHVAE performs worse than MIO, which just takes the likeliest out of 10 closest CEs. Further comparisons are in Appendix B.

5 Discussion and Conclusions

We have presented a comprehensive method for generating counterfactual explanations called LiCE. In section 3, we show that our method satisfies most common desiderata—namely validity, similarity, sparsity, actionability, causality, and most importantly, *plausibility*. We point to ways of including diversity and robustness, though we leave them for future work.

Our method shows promising performance in terms of plausibility, although time concerns are relevant once a full SPN is added to the model. We wish to stress that the MIO formulation of a Sum-Product Network opens up a variety of opportunities for further use.

Acknowledgements This work has received funding from the European Union’s Horizon Europe research and innovation program under grant agreement No. 101070568.

References

- [1] André Artelt and Barbara Hammer. Convex Density Constraints for Computing Plausible Counterfactual Explanations. In Igor Farkaš, Paolo Masulli, and Stefan Wermter, editors, *Artificial Neural Networks and Machine Learning – ICANN 2020*, volume 12396, pages 353–365. Springer International Publishing, Cham, 2020.
- [2] Andre Artelt, Valerie Vaquet, Riza Velioglu, Fabian Hinder, Johannes Brinkrolf, Malte Schilling, and Barbara Hammer. Evaluating Robustness of Counterfactual Explanations. In *2021 IEEE Symposium Series on Computational Intelligence (SSCI)*, pages 01–09, Orlando, FL, USA, December 2021. IEEE.
- [3] Barry Becker and Ronny Kohavi. Adult. UCI Machine Learning Repository, 1996. DOI: <https://doi.org/10.24432/C5XW20>.

- [4] Robert E Bixby. A brief history of linear and mixed-integer programming computation. *Documenta Mathematica*, 2012:107–121, 2012.
- [5] Francesco Bodria, Fosca Giannotti, Riccardo Guidotti, Francesca Naretto, Dino Pedreschi, and Salvatore Rinzivillo. Benchmarking and survey of explanation methods for black box models. *Data Mining and Knowledge Discovery*, pages 1–60, 2023.
- [6] Nadia Burkart and Marco F Huber. A survey on the explainability of supervised machine learning. *Journal of Artificial Intelligence Research*, 70:245–317, 2021.
- [7] Ruth M. J. Byrne. *The Rational Imagination: How People Create Alternatives to Reality*. The MIT Press, June 2005.
- [8] YooJung Choi, Antonio Vergari, and Guy Van den Broeck. Probabilistic circuits: A unifying framework for tractable probabilistic models. *UCLA*, October 2020.
- [9] Zhicheng Cui, Wenlin Chen, Yujie He, and Yixin Chen. Optimal Action Extraction for Random Forests and Boosted Trees. In *Proceedings of the 21th ACM SIGKDD International Conference on Knowledge Discovery and Data Mining*, pages 179–188, Sydney NSW Australia, August 2015. ACM.
- [10] Rudresh Dwivedi, Devam Dave, Het Naik, Smiti Singhal, Rana Omer, Pankesh Patel, Bin Qian, Zhenyu Wen, Tejal Shah, Graham Morgan, and Rajiv Ranjan. Explainable AI (XAI): Core Ideas, Techniques, and Solutions. *ACM Computing Surveys*, 55(9):194:1–194:33, January 2023.
- [11] Equal Credit Opportunity Act (ECOA). <https://www.law.cornell.edu/uscode/text/15/chapter-41/subchapter-IV>, 1974. Title 15 of the United States Code, Chapter 41, Subchapter IV, paragraph 1691 and following.
- [12] European Commission. Directive 2013/36/EU of the European Parliament and of the Council of 26 june 2013 on access to the activity of credit institutions and the prudential supervision of credit institutions and investment firms, amending Directive 2002/87/EC and repealing Directives 2006/48/EC and 2006/49/ec., 2016. Accessed: 2023-04-30.
- [13] European Commission. Regulation (EU) 2016/679 of the European Parliament and of the Council of 27 April 2016 on the protection of natural persons with regard to the processing of personal data and on the free movement of such data, and repealing Directive 95/46/EC (General Data Protection Regulation)., 2016. Accessed: 2023-04-30.
- [14] Robert Gens and Pedro Domingos. Learning the structure of sum-product networks. In *Proceedings of the 30th International Conference on International Conference on Machine Learning - Volume 28*, ICML’13, page III-873–III-880. JMLR.org, 2013.

- [15] Noam Goldberg, Steffen Rebennack, Youngdae Kim, Vitaliy Krasko, and Sven Leyffer. MINLP formulations for continuous piecewise linear function fitting. *Computational Optimization and Applications*, 79(1):223–233, May 2021.
- [16] Riccardo Guidotti. Counterfactual explanations and how to find them: Literature review and benchmarking. *Data Mining and Knowledge Discovery*, April 2022.
- [17] David Gunning. Broad agency announcement explainable artificial intelligence (xai). Technical report, DARPA, August 2016.
- [18] Gurobi Optimization, LLC. Gurobi optimizer reference manual, 2023.
- [19] Gurobi Machine Learning. Gurobi Optimization, January 2024.
- [20] Joey Huchette, Gonzalo Muñoz, Thiago Serra, and Calvin Tsay. When deep learning meets polyhedral theory: A survey. *arXiv preprint arXiv:2305.00241*, 2023.
- [21] Junqi Jiang, Francesco Leofante, Antonio Rago, and Francesca Toni. Formalising the robustness of counterfactual explanations for neural networks. *Proceedings of the AAAI Conference on Artificial Intelligence*, 37(12):14901–14909, June 2023.
- [22] Michael I Jordan, Zoubin Ghahramani, Tommi S Jaakkola, and Lawrence K Saul. An introduction to variational methods for graphical models. *Learning in graphical models*, pages 105–161, 1998.
- [23] Kentaro Kanamori, Takuya Takagi, Ken Kobayashi, and Hiroki Arimura. DACE: Distribution-Aware Counterfactual Explanation by Mixed-Integer Linear Optimization. In *Proceedings of the Twenty-Ninth International Joint Conference on Artificial Intelligence*, pages 2855–2862, Yokohama, Japan, July 2020. International Joint Conferences on Artificial Intelligence Organization.
- [24] Amir-Hossein Karimi, Gilles Barthe, Bernhard Schölkopf, and Isabel Valera. A survey of algorithmic recourse: definitions, formulations, solutions, and prospects. *arXiv preprint arXiv:2010.04050*, 2020.
- [25] Amir-Hossein Karimi, Bernhard Schölkopf, and Isabel Valera. Algorithmic recourse: from counterfactual explanations to interventions. In *Proceedings of the 2021 ACM conference on fairness, accountability, and transparency*, pages 353–362, 2021.
- [26] Diederik P. Kingma and Max Welling. Auto-Encoding Variational Bayes, December 2022.
- [27] Bo Li, Peng Qi, Bo Liu, Shuai Di, Jingen Liu, Jiquan Pei, Jinfeng Yi, and Bowen Zhou. Trustworthy AI: From Principles to Practices. *ACM Computing Surveys*, 55(9):177:1–177:46, January 2023.
- [28] Divyat Mahajan, Chenhao Tan, and Amit Sharma. Preserving Causal Constraints in Counterfactual Explanations for Machine Learning Classifiers, June 2020.

- [29] Donato Maragno, Jannis Kurtz, Tabea E. Röber, Rob Goedhart, § Ilker Birbil, and Dick den Hertog. Finding Regions of Counterfactual Explanations via Robust Optimization, May 2023.
- [30] Kiarash Mohammadi, Amir-Hossein Karimi, Gilles Barthe, and Isabel Valera. Scaling Guarantees for Nearest Counterfactual Explanations. In *Proceedings of the 2021 AAAI/ACM Conference on AI, Ethics, and Society*, AIES '21, pages 177–187, New York, NY, USA, July 2021. Association for Computing Machinery.
- [31] Alejandro Molina, Antonio Vergari, Karl Stelzner, Robert Peharz, Pranav Subramani, Nicola Di Mauro, Pascal Poupart, and Kristian Kersting. Spflow: An easy and extensible library for deep probabilistic learning using sum-product networks, 2019.
- [32] Ramaravind Kommiya Mothilal, Amit Sharma, and Chenhao Tan. Explaining Machine Learning Classifiers through Diverse Counterfactual Explanations. In *Proceedings of the 2020 Conference on Fairness, Accountability, and Transparency*, pages 607–617, January 2020.
- [33] Christos H Papadimitriou. On the complexity of integer programming. *Journal of the ACM (JACM)*, 28(4):765–768, 1981.
- [34] Axel Parmentier and Thibaut Vidal. Optimal Counterfactual Explanations in Tree Ensembles. In *Proceedings of the 38th International Conference on Machine Learning*, pages 8422–8431. PMLR, July 2021.
- [35] Martin Pawelczyk, Klaus Broemann, and Gjergji Kasneci. Learning Model-Agnostic Counterfactual Explanations for Tabular Data. In *Proceedings of The Web Conference 2020*, WWW '20, pages 3126–3132, New York, NY, USA, April 2020. Association for Computing Machinery.
- [36] Martin Pawelczyk, Sascha Bielawski, Johannes van den Heuvel, Tobias Richter, and Gjergji Kasneci. CARLA: A python library to benchmark algorithmic recourse and counterfactual explanation algorithms, 2021.
- [37] Hoifung Poon and Pedro Domingos. Sum-product networks: A new deep architecture. In *2011 IEEE International Conference on Computer Vision Workshops (ICCV Workshops)*, pages 689–690, November 2011.
- [38] Rafael Poyiadzi, Kacper Sokol, Raul Santos-Rodriguez, Tijl De Bie, and Peter Flach. FACE: Feasible and Actionable Counterfactual Explanations. In *Proceedings of the AAAI/ACM Conference on AI, Ethics, and Society*, pages 344–350, February 2020.
- [39] Chris Russell. Efficient Search for Diverse Coherent Explanations. In *Proceedings of the Conference on Fairness, Accountability, and Transparency*, FAT* '19, pages 20–28, New York, NY, USA, January 2019. Association for Computing Machinery.

- [40] Berk Ustun, Alexander Spangher, and Yang Liu. Actionable Recourse in Linear Classification. In *Proceedings of the Conference on Fairness, Accountability, and Transparency*, pages 10–19, Atlanta GA USA, January 2019. ACM.
- [41] Sandra Wachter, Brent Mittelstadt, and Chris Russell. Counterfactual Explanations Without Opening the Black Box: Automated Decisions and the GDPR. *SSRN Electronic Journal*, 2017.
- [42] H Paul Williams. *Model building in mathematical programming*. John Wiley & Sons, 2013.
- [43] Laurence A Wolsey. *Integer programming*. John Wiley & Sons, 2020.
- [44] Riting Xia, Yan Zhang, Xueyan Liu, and Bo Yang. A survey of sum–product networks structural learning. *Neural Networks*, 2023.
- [45] Songming Zhang, Xiaofeng Chen, Shiping Wen, and Zhongshan Li. Density-based reliable and robust explainer for counterfactual explanation. *Expert Systems with Applications*, 226:120214, September 2023.

A Notation

Generally, notation follows these rules:

- Capital letters typically refer to amounts of something, as in classes, features, bins, etc. Exceptions are U , L , and F , which are taken from the original work [39].
- Caligraphic capital letters denote sets or continuous spaces.
- Small Latin letters are used as indices, variables, or parameters of the MIP formulation.
- Small Greek letters refer to hyperparameters of the LiCE formulation or parameters of the SPN (scope ψ , parameters θ).
- Subscript is used to specify the position of a scalar value in a matrix or a vector. When in parentheses, it specifies the index of a vector within a set.
- Superscript letters refer to a specification of a symbol with otherwise intuitively similar meaning. Except for \mathbb{R}^P , where P has the standard meaning of P -dimensional.
- A hat ($\hat{\cdot}$) symbol above a variable means that the variable is the output of the Neural Network $h(\cdot)$.
- A prime ($'$) symbol as a superscript of a variable means that the variable is a part of (or the output of) the counterfactual.
- In bold font are only vectors. When we work with a scalar value, the symbol is in regular font.

The specific meanings of symbols used in the article are shown in Tables 2 to 6. The symbols are divided into groups.

- Functions non-specific to our task (Table 2)
- Used indices (Table 3)
- LiCE (hyper)parameters that can be tuned (Table 4)
- Classification task and SPN symbols (Table 5)
- MIO formulation parameters and variables (Table 6)

B Further comparisons

In this section, we would like to discuss some results that could not fit into the article’s main body.

General function symbols	
$ \cdot $	Absolute value (if scalar) or size of the set
$[\cdot]$	Set of integers, $[N] = \{1, 2, \dots, N\}$
$\mathbb{1}\{\cdot\}$	Equal 1 if input is true, 0 otherwise
$\ \cdot\ _0$	ℓ_0 norm, number of non-zero elements
$2^{[P]}$	Set of all subsets of $[P]$

Table 2: General functions used

Indices	
j	Index of features, typically $j \in [P]$
(m)	Index of counterfactuals within a set \mathcal{C}_x , typically $m \in [M]$
n	A node of the SPN, $n \in \mathcal{V}$
i	Index of bins of a histogram in a leaf node (n), typically $i \in [B_n]$
a	A predecessor node (of node n) in the SPN, usually $a \in \mathcal{A}_n$
k	A class ($k \in [C]$) or categorical value ($k \in [K_j]$) index
e	Index of feature that is changed as an effect of causal relation R

Table 3: Symbols used as indices

Distance comparison Looking at the first two columns of Table 7, we notice that the proposed LiCE method produces very close counterfactuals. In fact, when considering common counterfactuals, LiCE generates the closest CE out of all methods. It might seem impossible that LiCE would generate closer CEs than MIO, given that LiCE formulation is a more constrained MIO formulation with the same objective. However, the increased distance of CEs generated by MIO is because we generate the ten closest and select the one with the highest likelihood, which is often not the closest overall.

Indeed, if we were to choose the closest counterfactual (see the method MIO - closest), we would obtain mean $\|\cdot\|_{1,\text{MAD}}$ distances of around 3.8 for both columns of common factuals. This choice would, however, decrease the log-density values by around 1 for the common factuals and by approximately 3 for all CEs. This would arguably make the plausibility of such counterfactuals notably worse, if not outright implausible.

Looking at the other methods, we notice that DiCE and VAE generate counterfactuals that are very distant from their factuals. This further points to issues of the DiCE method, which has the only upside in it being able to generate a valid counterfactual most often. For VAE, on the other hand, this is a major disadvantage, as this method produced CEs of high quality in terms of plausibility. In other words, while this method produces plausible CEs (though often non-actionable), it generates them quite far away. So even though such a counterfactual might be plausible, the “road” to get there is long.

The other method utilizing an autoencoder, C-CHVAE, also performs poorly (though not as poorly as VAE) in terms of distance. It generates almost twice as close CEs com-

LiCE (hyper)parameters	
σ	Desired sign of counterfactual for binary classification. $\sigma = -1$ corresponds to class 0 and $\sigma = 1$ to class 1.
τ	The minimal difference between counterfactual class ($h^{\text{raw}}(\mathbf{x}')_{\hat{y}'}$) and factual class ($h^{\text{raw}}(\mathbf{x}')_{\hat{y}}$) NN output value. Alternatively, for binary classification, it is the requirement for minimal absolute value of the NN output before sigmoid activation ($h^{\text{raw}}(\mathbf{x}')$).
ρ	Limit for relative difference of values of the objective function within the set of closest counterfactuals $\mathcal{C}_{\mathbf{x}}$.
ϵ_j	Minimal change in continuous value c_j of j -th feature. The absolute difference between x'_j and x_j is either 0, or at least ϵ_j .
δ^{SPN}	Lower bound on estimated value of likelihood of the generated counterfactual.

Table 4: Input parameters into the LiCE formulation

pared to VAE. Nevertheless, they are still farther than the CEs of the rest of the methods (except those mentioned).

FACE seems to be performing very well in terms of distance, especially the results on all factuals look promising. Unfortunately, one must be careful when comparing those since the means are computed on different sets of factual instances. The distance differences are rather small, comparing the LiCE, MIO, and FACE counterfactuals. Considering that the results of *MIO - closest* are globally optimal on the factuals it succeeded on, we can assume that both FACE and LiCE can generate sufficiently close CEs. While FACE has a slight advantage in the distance measure, it performs worse in success rate and plausibility, as addressed before.

Sparsity comparison Coming to sparsity, we compare the mean number of changes to a factual in Table 8. The results are correlated to the distances. DiCE and VAE again perform the worst, while C-CHVAE is closely third from the back in all four columns.

MIO approach utilizing the $\|\cdot\|_{1,\text{MAD}}$ as a measure of distance generates the most sparse CEs. This dominance is even clearer when considering the counterfactuals closest to the factual.

Regarding the sparsity of LiCE, there is room for improvement. We can see that a constraint in Eq. 10 with $S = 3$ might be beneficial since it seems that there usually is a counterfactual with the number of changes ≤ 3 , although it might also lead to lower success rate of generating a valid counterfactual. Selecting the closest CE generated by LiCE instead of the likeliest, similarly to the presented MIO, does not improve sparsity as much, only by about 0.1.

FACE has very low mean sparsity, similar to MIO, though it has notably higher variance. Considering its results in terms of distance and log-density (plausibility), FACE method performs quite well on the task of generating CEs with multiple objectives in mind. A deeper comparison would be an intriguing area of future research.

Classification task symbols	
P	Number of features
C	Number of classes
\mathcal{D}	The dataset, set of 2-tuples $(\mathbf{x}, y) \in \mathcal{D}$
\mathcal{X}	Input space $\mathcal{X} \subseteq \mathbb{R}^P$
\mathbf{x}	A (factual) sample $\mathbf{x} \in \mathcal{X}$
x_j	A j -th feature of sample \mathbf{x}
y	Ground truth of sample \mathbf{x} , $y \in [C]$
$h(\cdot)$	Classifier we are explaining $h : \mathcal{X} \rightarrow [C]$
\hat{y}	Classifier-predicted class $h(\mathbf{x}) = \hat{y} \in [C]$
$h^{\text{raw}}(\cdot)$	NN classifier output without activation $h^{\text{raw}} : \mathcal{X} \rightarrow \mathcal{Z}$
\mathcal{Z}	Output space of the NN classifier, without sigmoid/softmax activation
Counterfactual generation symbols	
$\ \cdot\ _{1,\text{MAD}}$	Counterfactual distance function (see Eq. 9)
$\mathcal{C}_{\mathbf{x}}$	Set of generated counterfactuals for factual \mathbf{x}
M	Number of sought counterfactuals, $M \geq \mathcal{C}_{\mathbf{x}} $
\mathbf{x}'	Counterfactual explanation of \mathbf{x} , $\mathbf{x}' \in \mathcal{C}_{\mathbf{x}}$
\mathbf{x}'^*	Optimal (closest) counterfactual
$\mathbf{x}'_{(m)}$	m -th counterfactual explanation of factual \mathbf{x}
x'_j	A value of j -th feature of the counterfactual
\hat{y}'	Predicted class of the counterfactual (can be a parameter of LiCE)
Sum Product Network symbols	
\mathcal{V}	Set of nodes of the SPN
\mathcal{V}^L	Set of leaf nodes
\mathcal{V}^Σ	Set of sum nodes
\mathcal{V}^Π	Set of product nodes
$\text{pred}(\cdot)$	Function returning children (predecessors) of a node
$\psi(\cdot)$	Scope function mapping nodes to their input features $\psi : \mathcal{V} \rightarrow 2^{[P]}$
θ	Parameters of the SPN
O_n	Output value of a node $n \in \mathcal{V}$
$w_{a,n}$	Weight of output value of predecessor node a in computing the value of sum node n .
n^{root}	Root node, its value is the value of the SPN

Table 5: Symbols of the classification task, CE search, and SPNs

MIO formulation variables	
l_j	Decrease in continuous value of j -th feature.
\mathbf{l}	Concatenated vector of all l_j .
u_j	Increase in continuous value of j -th feature.
\mathbf{u}	Concatenated vector of all u_j .
c_j	Continuous value of j -th CE feature.
$d_{j,k}$	1 iff x'_j takes k -th categorical value $k \in K_j$.
\mathbf{d}	All variables $d_{j,k}$ concatenated into a vector.
d_j^{cont}	1 iff x'_j takes continuous value c_j .
$h^{\text{raw}}(\cdot)_k$	Value of h^{raw} , corresponding to class $k \in [C]$.
g_k	1 iff class $k \in [C]$ has higher h^{raw} value than the factual class.
s_j	1 iff j -the feature changed, i.e., $x_j \neq x'_j$.
r	1 iff causal relation R is activated, i.e., cause is satisfied and effect is enforced.
$\bar{b}_{n,i}$	1 iff x'_j does <i>not</i> belong to the i -th bin ($i \in [B_n]$), assuming j -th feature corresponds to node n , i.e., $\psi(n) = \{j\}$.
o_n	Estimated output value of SPN node $n \in \mathcal{V}$.
MIO formulation parameters	
L_j	Lower bound on continuous values of j -th feature. In our implementation equal to 0.
U_j	Upper bound on continuous values of j -th feature. In our implementation equal to 1.
F_j	Default continuous value of j -th feature, equal to the value of the factual x_j , if it has continuous value. Otherwise equal to median.
K_j	Number of categorical values of j -th feature.
f_j	Equal to x_j , if it has categorical value. If x_j continuous, f_j is removed and so are all constraints containing it.
S	Maximal number of feature value changes of \mathbf{x}' compared to \mathbf{x} . Sparsity limit.
R	Example causal relation: if j -th feature increases, e -th feature must decrease.
B_n	Number of bins in histogram of leaf node n .
$t_{n,i}$	Threshold between $i-1$ -th and i -th bin in histogram of leaf node n
$q_{n,i}$	Likelihood value of i -th bin of node n .
\mathcal{A}_n	Set of predecessors of node n , $\mathcal{A}_n = \text{pred}(n)$.
\mathbf{v}^{bin}	Vector of respective $\ \cdot\ _{1,\text{MAD}}$ weights for binary one-hot encodings.
\mathbf{v}^{cont}	Vector of respective $\ \cdot\ _{1,\text{MAD}}$ weights for continuous values.
\mathbf{d}^{fact}	One-hot encoded vector of factual categorical values corresponding to \mathbf{d} .

Table 6: Used variables and parameters in the MIO formulation

Method	$\ \cdot\ _{1,\text{MAD}}$ on common factuals		$\ \cdot\ _{1,\text{MAD}}$ on all factuals	
	Valid (17%)	Actionable (7%)	Valid	Actionable
DiCE	16.65 ± 4.79	17.54 ± 4.21	17.99 ± 5.05	18.00 ± 5.05
VAE	14.59 ± 4.05	13.65 ± 2.67	18.02 ± 5.27	15.29 ± 4.40
FACE (ϵ)	6.79 ± 4.48	6.33 ± 3.83	7.39 ± 5.95	6.59 ± 5.83
FACE (knn)	7.07 ± 4.74	6.66 ± 3.58	8.08 ± 5.99	7.15 ± 5.77
C-CHVAE	8.19 ± 4.23	7.98 ± 4.27	10.41 ± 4.83	10.48 ± 4.77
MIO - likeliest	5.41 ± 2.41	5.53 ± 2.46	6.62 ± 2.70	6.63 ± 2.70
<i>MIO - closest</i>	3.79 ± 2.33	3.83 ± 2.37	5.23 ± 2.77	5.24 ± 2.77
LiCE	4.98 ± 3.36	4.72 ± 2.61	7.41 ± 4.48	7.41 ± 4.48

Table 7: The mean distance of a counterfactual to its respective factual, measured using the $\|\cdot\|_{1,\text{MAD}}$ function, described in Eq. 9. *MIO - closest* is an extra row that represents counterfactuals generated by the MIO formulation if we took the closest one instead of the one with the highest likelihood out of 10. The last two columns are computed on all factuals the method was able to generate a valid/actionable CE. The relative amounts are shown in Table 1. The values computed on all factuals are difficult to compare directly since the means are computed on different sets of factuals, based on which factuals led to a successful generation of counterfactuals.

Further comments on plausibility To elaborate further on the plausibility measures, we restate our objective in terms of the log-density obtained by KDE. We wish to obtain counterfactuals that have a high enough likelihood of being from the same distribution as the training data. We estimate this using the SPN during the CE search and test the results using a separate KDE model, similar to [1].

This resemblance of points in the data can be assessed using an out-of-sample *median* log-density of KDE and comparing it to the log-densities of generated counterfactuals. We take the median because we wish to be robust to outlier samples. However, we compare the *mean* log-densities of generated counterfactuals because we should not generate outliers. This attribute of not being an outlier is often considered the definition of the plausibility of CEs [16, 23].

If we compare the results to the *median* log-density on the test set (-12.64), we see that only LiCE (and possibly VAE) achieve comparable values consistently. Were we to compare the methods to the *mean* log-density on the test set, which equals -14.16 , the FACE method performs comparably. This might be caused by the FACE method selecting outlier samples from the training set.

It would be interesting to compare the FACE method on a pruned set of training samples. For example, we could remove the bottom 10% of samples in terms of SPN estimated likelihood from the training set and then use the FACE method.

Method	# of changes on common factuals		# of changes on all factuals	
	Valid (17%)	Actionable (7%)	Valid	Actionable
DiCE	3.85 ± 1.07	3.92 ± 1.01	4.19 ± 1.04	4.19 ± 1.04
VAE	4.08 ± 0.95	3.89 ± 0.87	4.90 ± 1.20	4.15 ± 0.93
FACE (ϵ)	2.46 ± 0.76	2.47 ± 0.64	2.25 ± 1.36	2.07 ± 1.42
FACE (knn)	2.41 ± 0.79	2.44 ± 0.68	2.43 ± 1.34	2.19 ± 1.36
C-CHVAE	3.41 ± 0.91	3.44 ± 1.01	3.76 ± 0.86	3.80 ± 0.88
MIO	2.21 ± 0.88	2.33 ± 0.85	2.48 ± 0.89	2.49 ± 0.89
<i>MIO - closest</i>	1.69 ± 0.67	1.75 ± 0.64	2.03 ± 0.89	2.03 ± 0.89
LiCE	2.79 ± 0.84	2.81 ± 0.78	3.33 ± 1.01	3.33 ± 1.01

Table 8: We compare sparsity, measured as a mean number of changed feature values of the factual, to obtain the counterfactual. *MIO - closest* is an extra row that represents counterfactuals generated by the MIO formulation if we took the closest one instead of the one with the highest likelihood out of 10. The last two columns are computed on all factuals the method was able to generate a valid/actionable CE. The relative amounts are shown in Table 1. The values computed on all factuals are difficult to compare directly since the means are computed on different sets of factuals, based on which factuals led to a successful generation of counterfactuals.

C Additional comments on experiments

We use a simplified variant of the Adult dataset. It contains six categorical variables (work class, education, marital status, occupation, gender, and race) and two continuous (age and working hours per week). We predict the original target feature income. The dataset has no missing values and contains 32 561 samples. This dataset was used in the original implementation of [39].

We compare methods on a neural network with four layers, with size 29 (length of the encoded input) on the input, then 15 and 10 for hidden layers, and one neuron as output. We compare all methods on this neural network architecture, trained five times for each training set (from the five folds) separately. We include both classes in the selection of 100 testing samples since we test the general capabilities rather than showcase a realistic scenario.

We compare our method to some publicly available implementations of competing methods. Since the experimental part serves mostly as an illustration, we did not tune hyperparameters (except for the testing Kernel Density Estimator) but used default ones. If no default was set, we picked reasonable values. We would ideally compare the LiCE method to the DACE [23] method; however, its public implementation works with a single hidden layer and thus could not be compared to other methods directly as is.

Many comparisons are worth exploring, but we leave them for future work.